—Original—

Effects of ketoconazole on cyclophosphamide metabolism: evaluation of CYP3A4 inhibition effect using the *in vitro* and *in vivo* models

Le YANG[1]*, Chenyang YAN[2]*, Feng ZHANG[1], Bo JIANG[1], Shouhong GAO[1], Youtian LIANG[1], Lifeng HUANG[1], and Wansheng CHEN[1]

[1])Department of Pharmacy, Changzheng Hospital, Second Military Medical University, No. 415, Fengyang Road, Shanghai 200003, P.R. China
[2])Department of Quality Management, Changzheng Hospital, Second Military Medical University, No. 415, Fengyang Road, Shanghai 200003, P.R. China

Abstract: Cyclophosphamide (CP) is widely used in anticancer therapy regimens and 2-dechloroethylcyclophosphamide (DECP) is its side-chain dechloroethylated metabolite. N-dechloroethylation of CP mediated by the enzyme CYP3A4 yields nephrotoxic and neurotoxic chloroacetaldehyde (CAA) in equimolar amount to DECP. This study aimed to evaluate the inhibitory effect of ketoconazole (KTZ) on CP metabolism through *in vitro* and *in vivo* drug-drug interaction (DDI) research. Long-term treatment of KTZ induces hepatic injury; thus single doses of KTZ at low, middle, and high levels (10, 20, and 40 mg/kg) were investigated for pharmacokinetic DDI with CP. Our *in vitro* human liver microsome modeling approach suggested that KTZ inhibited CYP3A4 activity and then decreased DECP exposure. In addition, an UHPLC-MS/MS method for quantifying CP, DECP, and KTZ in rat plasma was developed and fully validated with a 4 min analysis coupled with a simple and reproducible one-step protein precipitation. A further *in vivo* pharmacokinetic study demonstrated that combination use of CP (10 mg/kg) and KTZ (10, 20, and 40 mg/kg) in rats caused a KTZ dose-dependent decrease in main parameters of DECP (C_{max}, T_{max}, and $AUC_{0-\infty}$) and provided magnitude exposure of DECP (more than a 50% AUC decrease) as a consequence of CYP3A inhibition but had only a small effect on the CP plasma concentration. Our results suggested that combination usage of a CYP3A4 inhibitor like KTZ may decrease CAA exposure and thus intervene against CAA-induced adverse effects in CP clinical treatment.
Key words: 2-dechloroethylcyclophosphamide, cyclophosphamide, drug-drug interaction, ketoconazole, UHPLC-MS/MS

Introduction

Cyclophosphamide (CP) is an alkylating oxaza-phosphorine anticancer agent routinely used in treatment of a variety of pediatric and adult tumors, such as soft tissue sarcomas and lymphomas [13, 21, 22]. It is an inactive prodrug that requires enzymatic and chemical activation: CP is primarily biotransformed to 4-hydrox-
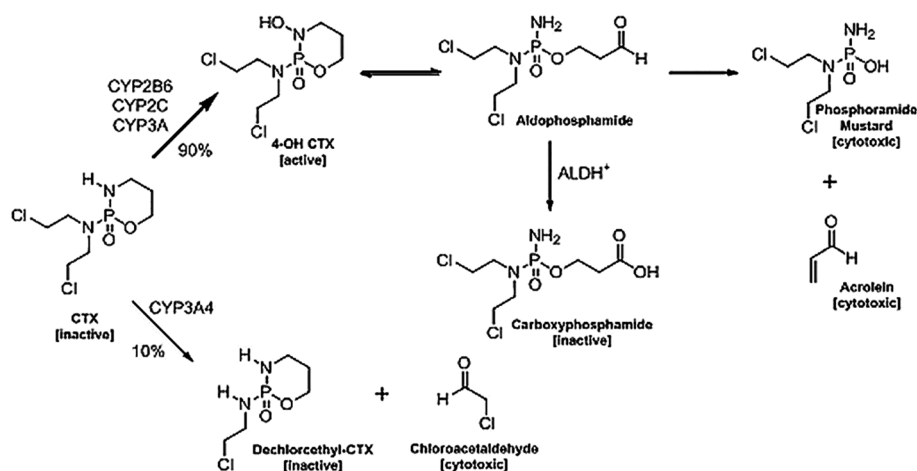
Fig. 1. Metabolic scheme of CP.

ycyclophosphamide (4-OH CP) and aldophosphamide in the liver by cytochrome P450 (CYP450) enzymes, and then aldophosphamide was catalyzed to acrolein through β-elimination, yielding the ultimate alkylating metabolite that accounts for its cytotoxic properties, phosphoramide mustard. Meanwhile, about 10% of CP was partly dechloroethylated to give equivalent amounts of 2-dechloroethylcyclophosphamide (DECP) and chloroacetaldehyde (CAA), and CYP3A4 exhibited the highest *N*-dechloroethylation activity toward this pathway (Fig. 1) [4, 5, 20]. Attaining therapeutic versus toxic outcomes in patients treated with CP requires an understanding of the individual variation in both activation and detoxifying pathways [11]. Among these metabolites, acrolein is known to be responsible for the hemorrhagic cystitis observed in some patients, whereas CAA is said to be responsible for nephrotoxicity and neurotoxicity [20, 27]. In order to prevent hemorrhagic cystitis caused by acrolein, 2-mercaptoethane sulfonate (MESNA) is coadministered to patients currently being prescribed CP. However, MESNA cannot reduce CAA nephrotoxicity *in vivo* [27].

Using protective agents to intervene against toxicities may help to withstand the side effects associated with acrolein in CP treatment [27], and another option could be to apply a CYP3A4 inhibitor against CAA-induced side effects. A draft guidance of the US FDA recommends that ketoconazole (KTZ), a strong inhibitor of CYP3A4, be used to evaluate, through study of pharmacokinetic parameter changes, potential drug-drug interaction (DDI) with new molecular entities that are substrates of CYP3A4 because coadministration with KTZ

can result in an increased plasma concentration, prolonged pharmacologic action of these agents, and thus increased the risk of drug-related adverse events [43]. For example, KTZ has been investigated for concomitant administration with mirodenafil, bortezomib, gemigliptin, bosutinib, and almorexant in healthy volunteers or patients, and a corresponding drug exposure has been achieved as a result of CYP3A4 inhibition [1, 11, 30, 34, 39]. Since CYP3A4 plays a predominant role in CP's decloroethylation pathway, coadministration of CP and KTZ may induce occurrence of DDI.

KTZ possesses toxicity in mammalian cells and tissues when used in higher orally therapeutic doses, which were reported to be about 800 to 1,200 mg/day for humans and 300 mg/kg/day during 14 consecutive days [32, 33, 36]. In our study, single doses of KTZ at low, middle, and high levels (10, 20, and 40 mg/kg) were investigated for pharmacokinetic DDI with CP, and KTZ application was recognized to be relatively tolerable.

It is important to predict DDI risks in humans based on *in vitro* data and modeling of pharmacokinetics, and several *in vitro* approaches have been established [28]. In our previous study, the human liver microsomes (HLM) approach, a valuable *in vitro* tool in many laboratories, was applied to investigate the potential inhibitory effects of 21 main compounds from a traditional Chinese medicine on CYP1A2, 2C9, 2C19, 2D6, 2E1, and 3A4 [9]. Moreover, an *in vivo* rat model provides information regarding the overall hepatic disposition, which is influenced by the coadministered drug, and also potential DDI information [3, 19, 26].

Previously, we reported an ultra-high-pressure liquid

chromatography-tandem mass spectrometry (UHPLC-MS/MS) method to determine CP and DECP in rat plasma and revealed that monitoring of an *N*-dechloroethylation metabolite (DECP) could indirectly quantify the equimolar CAA [43]. In this study, we constructed a simultaneous pharmacokinetic investigation by a newly established UHPLC-MS/MS method for CP, DECP, and KTZ assay in rats, after examining the inhibitory effect of KTZ on the HLM model. By using the *in vitro* and *in vivo* models, the CYP3A4 inhibition effect of KTZ on the CP metabolism was evaluated for the first time. This study also provided scientific data for a therapeutic intervention based on a CYP3A4 inhibitor against the adverse effects caused by CAA in CP clinical treatment.

Materials and Methods

Chemicals and reagents

A human liver was obtained from the Organ Transplantation Institute of PLA, Changzheng Hospital, and used for the tissues in a xenobiotic metabolism study after approval by the Ethics Committee of the Shanghai Changzheng Hospital (Shanghai, China). Protein contents of the hepatic microsomes (HLM, 5 mg microsomal protein/ml) were measured by Bradford assay [7]. NADPH, glucose 6-phosphate, glucose-6-phosphate dehydrogenase, PBS, and Tris-HCl buffer were purchased from Sigma-Aldrich (St. Louis, MO, USA). NADPH-regenerating solution was prepared in a final concentration of 0.5 mg/ml NADPH, 10 mM glucose 6-phosphate, 0.8 U/ml glucose-6-phosphate dehydrogenase, and 5 mM MgCl$_2$.

CP (purity 99%), tinidazole (IS, purity 98%), KTZ (purity 98%), and 5% sodium carboxymethyl cellulose (CMC-Na, purity 99%) were purchased from the National Institute for the Control of Pharmaceutical and Biological Products (Beijing, China), DECP was provided by Toronto Research Chemicals (North York, ON, Canada, purity>97%), and acetonitrile (HPLC grade) was obtained from Merck (Darmstadt, Germany). Formic acid (purity 99%) was purchased from Tedia Co., Inc. (Fairfield, OH, USA). Ultrapure water was produced by a Milli-Q Reagent Water System (EMD Millipore, Billerica, MA, USA). Other reagents used in this study were of analytical grade.

Instrument

The samples were analyzed on an UHPLC-MS/MS

(Agilent Technologies, Wilmington, DE, USA) consisting of an Agilent 1290 UHPLC and Agilent 6460 triple-quadrupole mass spectrometer. The 1290 UHPLC system includes an autosampler, a binary pump, and a column oven, while the triple-quadrupole instrument was coupled with an electrospray ionization (ESI) source operated in a positive mode in this study. The MassHunter software from Agilent was used to obtain and analyze the data.

Chromatography and mass condition

Separation of the analytes was performed on a Waters HSS T3 C18 column (2.1 × 100 mm, 1.7 μm); the mobile phase consisted of acetonitrile (A) and 0.1% formic acid (B) at a flow rate of 0.5 ml/min, and the gradient program was set as follow: 0–4 min, 20% A to 90% A, post-run time, 2.5 min. The injection volume was 2 μl, and the autosampler temperature was maintained at 4°C. Multi-reaction mode (MRM) was selected to acquire the sample data. The capillary voltage was set at 3,500 V. The value for dwell time was 50 ms. The gas temperature and the sheath gas temperature were set at 325°C and 350°C, while the flows of drying gas and sheath gas were 10 l/min and 12 l/min.

Conversion of CP to DECP in HLM

The incubation mixture consisting of CP (160 mM, 50 μl), HLM (5 mg/ml, 50 μl), and PBS (50 μl) was preincubated for 5 min at 37°C. The reaction was initiated with the NADPH-regenerating solution in 200 μl of Tris-HCl buffer and terminated at 5 min, 15 min, 30 min, 60 min, and 90 min by adding 400 μl of ice-cold acetonitrile containing internal standard tinidazole (100 ng/ml). Incubations lacking NADPH served as negative controls. Samples were centrifuged at 14,000 g for 10 min. A 2 μl aliquot of the supernatant was analyzed by a developed LC-MS/MS method [43].

Determination of type of inhibition

To further investigate the inhibition of CYP3A4 activity by KTZ enzyme inhibition kinetic experiments were carried out with KTZ in the range of 0.01–10.00 μM. A later inhibition study was performed with four concentrations of KTZ and five concentrations of CP. A $P<0.05$ was considered to indicate a significant statistical difference between the control and test groups.

Calibration standards and quality control (QC) samples

Stocking solutions of CP, DECP, IS, and KTZ were

prepared separately at 1 mg/ml in methanol. All solutions were stored at −20°C until use. On each day of analysis, calibration standards and QC samples were newly prepared in 90 μl rat blank plasma by adding a 10 μl of corresponding working solutions to give eight standards ranging from 10 to 1,000 ng/ml for CP and DECP from 5 to 500 ng/ml for KTZ and three QCs at 20, 80, and 500 ng/ml for CP and DECP and at 10, 40, and 250 ng/ml for KTZ.

Sample pretreatment

Protein precipitation was chosen for the sample pretreatment. Calibration, QC, and clinical samples (100 μl) were pretreated in 1.5 ml polypropylene tubes using 300 μl acetonitrile containing 0.1% formic and IS (200 ng/ml). After vortex mixing for 1 min, the plasma samples were centrifuged at room temperature at 12,000 rpm for 10 min. Then 2 μl of the supernatant was injected for UHPLC-MS/MS analysis.

Method validation

This quantitative UHPLC-MS/MS method was validated in terms of specificity, linearity, lower limit of quantitation (LLOQ), accuracy and precision, matrix effect and extraction recovery, dilution effect, and the incurred sample reanalysis test by referring to the US FDA Guidance for Industry Bioanalytical Method Validation.

Specificity was investigated by comparing the chromatograms of six different batches of rat plasma with the corresponding plasma sample spiked with a known amount of CP, DECP, KTZ, and IS.

Calibration curves were achieved at eight points in rat plasma, ranging from 10 to 1,000 ng/ml for both CP and DECP and from 5 to 500 ng/ml for KTZ. Least-squares regression function was fitted by weighting 1/x of the analyte/IS peak area ratio versus the nominal analyte concentration relationship to construct the daily calibration curves. Three duplicates were performed for each point, and each point was analyzed for three consecutive days. The LLOQ was the lowest point of the calibration curve, which can be determined with accepted precisions and accuracies, which were less than 20%, and its signal-to-noise ratio (S/N) should be more than 10.

QC samples (CP and DECP, 20, 80, and 500 ng/ml; KTZ, 10, 40, and 250 ng/ml) were prepared and analyzed on one day (intraday precision) and three consecutive days (interday precision). Five duplicates were prepared

for each point. Accuracy was calculated as the ratio of the measured concentration to the nominal concentration multiplied by 100%, while the precision was the bias of the different measured concentrations. Precision and accuracy were expressed by the coefficient of variation (CV,%) and relative error (RE,%).

To evaluate the matrix effect, the peak area of each analyte from the post-spiked samples at the different QC levels was compared to its corresponding working solution at the same level. Extraction recovery was calculated for CP, DECP, and KTZ as the ratio of the analyte peak area from the extracted QC sample to the extracted blank plasma post-spiked with the corresponding working solution.

As a preliminary study showed that the concentrations of CP and KTZ in some plasma samples were higher than the upper limit of quantification (ULOQ), dilution effect was taken into consideration. Quality control samples (10 μl) spiked with 2,000 ng/ml CP, and 1,000 ng/ml KTZ were diluted using blank plasma in five duplicates. Accuracy was determined as the percentage deviation of the calculated concentrations from the nominal concentration, and REs should be less than 10%.

Stability assessments were performed for short-term (25°C for 3 h), long-term (−80°C for 3 months), and three freeze-thaw cycle stabilities (−80°C to 25°C). REs should be less than 15%.

Incurred sample reanalysis (ISR) was conducted using randomly selected rat plasma samples. In general, 10% of samples should be reanalyzed, and the samples should be reanalyzed, and the samples should be around the maximal concentration C_{max} and in the elimination phase. RE was applied for ISR estimation by using the following formula, and it should not be more than ± 20% [16].

$$RE = \frac{\text{reanalysis value - original value}}{\text{mean of reanalysis value and original value}} \times 100\%$$

Pharmacokinetic study design and incurred sample reanalysis

SPF male SD rats (180–220 g) obtained from the Animal Center of the Second Military Medical University, Shanghai, China, were kept under regulated environmental conditions (temperature, 25 ± 2°C; humidity, 60 ± 5%; 12 h dark/light cycle), and food was withheld overnight. Animal experiments were reviewed and approved by the Ethics Committee of Changzheng Hospital, Shanghai, China.

Table 1. KTZ inhibition of CP conversion to DECP in HLM

KTZ concentration (μM)	DECP concentration (n=3, ng/ml)				
	1	2	3	Average	SD
0.01	14.03	12.77	13.78	13.53	0.67
0.10	16.86	18.36	13.42	16.21	2.53
0.50	16.74	12.8	13.23	14.26	2.16
1.00	9.74	10.07	9.02	9.61	0.54
2.00	3.69	2.86	2.12	2.89	0.79
5.00	1.77	1.89	2.07	1.91	0.15
10.00	1.29	1.38	1.12	1.26	0.13

All animals were randomly separated into five groups (n=6). Rats in group 0 were orally administered with KTZ (20 mg/kg). Rats in group 1 were pretreated with an equal volume of 5% CMC-Na and then intravenously administered CP 50 min later (10 mg/kg, i.v.). Rats in group 2 were administered with CP (10 mg/kg, i.v.) 50 min following an oral dosage of 10 mg/kg KTZ [30]. Rats in group 3 were administered with CP (10 mg/kg, i.v.) 50 min following an oral dosage of 20 mg/kg KTZ. Finally, rats in group 4 were administered CP (10 mg/kg, i.v.) 50 min following an oral dosage of 40 mg/kg KTZ. Drugs were suspended in in 2 ml of 5% CMC-Na for oral administration or in 2 ml of saline for intravenous administration.

After drug administration, 300 μl blood samples were collected from orbit at different time intervals (0.083, 0.166, 0.25, 0.5, 1, 1.5, 2, 3, 4, 6, 8, 12, and 24 h). Plasma samples were separated by centrifugation at 4,000 rpm for 10 min and stored at −20°C until analysis. All pharmacokinetic parameters were processed by Drug and Statistics 2.0 (Mathematical Pharmacology Professional Committee of China, Shanghai, China) using a compartmental pharmacokinetic analysis model.

Results

CP metabolism by HLM and the inhibition effect from KTZ

Based on the LC-MS/MS assay for CP and DECP, DECP exhibited its maximum amount through CYP3A4 metabolism after incubation with HLM for 60 min, with the Km value being 160 mM for CP (Supplementary Fig. 1). As a strong inhibitor of CYP3A4, it was found that addition of KTZ to the incubation of CP with HLM greatly reduced the DECP production (Table 1), and the IC_{50} value for the KTZ concentration was 0.618 μM when KTZ decreased the CYP3A4 activity of HLM
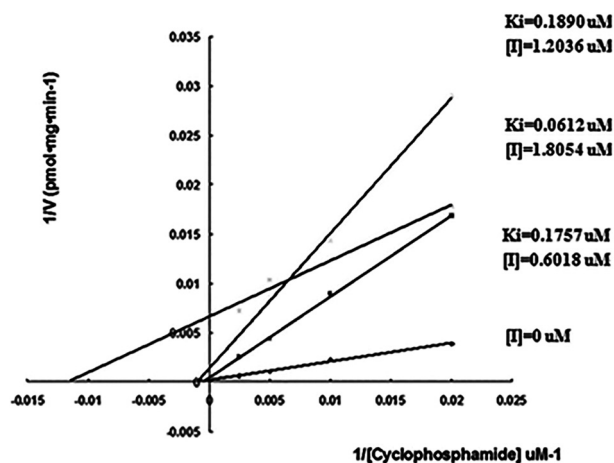

Fig. 2. Lineweaver-Burk plot for CYP3A4 inhibition by KTZ in HLM at different concentrations of KTZ (n=3).

(Supplementary Fig. 2). A later inhibition study was performed with four concentrations of KTZ (0, 0.618, 1.2036, and 1.8504 μM) and five concentrations of CP (50, 100, 200, 400, and 800 μM). Based on analysis of nonlinear regression of inhibition data and a primary Lineweaver-Burk plot and secondary plot presented in HLM, the KTZ inhibition of CYP3A4 activity appeared to be noncompetitive when the concentration of KTZ was below 1.850 μM (3 times of the IC_{50}) and anticompetitive when it was above 1.850 μM (Fig. 2). The inhibition constant (Ki) values for KTZ were 0.1757, 0.0612, and 0.1890 μM at three different concentrations: 0.618, 1.2036, and 1.8504 μM (Supplementary Fig. 2).

Validation of method

Specificity: Specificity was used to evaluate the ability of the method to separate and quantitate the analytes in the presence of other biological endogenous constituents and to detect potential interferences like ion suppression or enhancement. The mass transitions for CP, DECP,

Table 2. Accuracy and precision for DECP, CP, and KTZ

Analyte	Nominal Concentration (ng/ml)	Intraday (n=5)			Interday (n=15)		
		Measured (ng/ml)	RE (%)	CV (%)	Measured (ng/ml)	RE (%)	CV (%)
DECP	10 (LLOQ)	9.90 ± 0.48	−0.96	4.81	10.22 ± 0.61	2.22	5.95
	20	20.40 ± 0.65	2.01	3.18	20.92 ± 0.87	4.61	4.15
	80	83.49 ± 2.00	4.36	2.40	87.54 ± 4.51	9.42	5.15
	500	539.10 ± 56.36	7.82	10.46	527.44 ± 45.86	5.49	8.69
CP	10 (LLOQ)	9.24 ± 0.13	−7.65	1.44	9.59 ± 0.43	−4.06	4.49
	20	18.77 ± 0.16	−6.17	0.83	19.71 ± 0.88	−1.47	4.48
	80	78.705 ± 1.14	−1.62	1.45	82.50 ± 2.17	3.13	2.641
	500	555.36 ± 48.09	11.07	8.66	515.51 ± 22.08	3.10	4.28
KTZ	5 (LLOQ)	4.96 ± 0.12	−0.87	2.39	5.01 ± 0.11	0.23	2.23
	10	9.66 ± 0.12	−3.38	1.28	9.78 ± 0.28	−2.24	2.84
	40	39.64 ± 0.60	−0.89	1.51	40.41 ± 1.45	1.02	3.60
	250	254.65 ± 28.96	1.86	11.37	254.01 ± 20.07	1.60	7.90

IS, and KTZ were m/z 261 → 140, 199 → 78, 248 → 121, and 531.2 → 82, respectively (Supplementary Fig. 3). Supplementary Fig. 4 shows the typical UHPLC-MS/MS chromatograms for a blank plasma, a plasma sample pre-spiked with CP (200 ng/ml), DECP (200 ng/ml), IS (50 ng/ml) and KTZ (100 ng/ml), and a rat plasma sample from group 2 (1 h after dosing with CP). No interference in the blank plasma traces was observed from other endogenous substances in this method.

Linearity and LLOQ: Linearity was evaluated by analyzing eight calibration standards in duplicates over the concentration ranges of 10–1,000 ng/ml for both CP and DECP and 5–500 ng/ml for KTZ. The correlation coefficients (R^2) obtained using $1/x^2$ weighted linear regressions were better than 0.99 for CP, DECP, and KTZ. LLOQ was defined as the lowest concentration with precision and accuracy less than 15%. The intraday assay yielded acceptable precisions of 4.81% (CV) for DECP and 1.44% (CV) for CP and accuracies of −0.96% (RE) for DECP and −7.65% (RE) for CP (Table 2).

Precision and accuracy: Precision and accuracy were analyzed at low, medium, and high levels of QC samples. The detailed data showed that the intra- and interday precisions (CVs) were lower than 15%, with accuracies (REs) in the range of −7.65% to 11.07% for all analytes (Table 2), which demonstrated that the current method fulfilled the requirement of the FDA Guidance.

Matrix effect and extraction recovery: Matrix effect data from three QC levels of CP, DECP, and KTZ in five different batches of rat blank plasma are presented in Table 3. All data were within the acceptable range of 96.39% to 107.59%, with CVs<10%, indicating absence of the relative matrix effect for analytes in rat plasma.

The mean extraction recoveries of CP, DECP, and KTZ were 100.04 ± 1.04% − 100.83 ± 0.49%, 99.41 ± 0.36% − 101.82 ± 3.52%, and 94.35 ± 2.31% − 97.73 ± 0.44%, respectively (Table 3), indicating this method was highly reproducible.

Dilution effect: For the dilution test, an additional QC sample was prepared at 2,000 ng/ml for CP and DECP and at 1,000 ng/ml for KTZ, and it was then diluted 1:10 (v/v) in blank rat plasma before mass spectrometry (MS) analysis. Accuracy (RE) and precision (CV) were 96.17% and 1.69% for CP, 96.75% and 2.45% for DECP, and 98.62% and 2.17% for KTZ.

Stability test: Stability experiments for CP, DECP, and KTZ in controlled samples of rat plasma were analyzed under three different sets of conditions: 25°C for 3 h (short-term stability), −80°C for 3 months long-term stability), and −80°C to 25°C (stability in the three freeze-thaw cycles). All data are shown in Table 4, which indicates that CP, DECP, and KTZ proved to be stable throughout the whole manipulation and storage processes.

ISR analysis: Reanalysis was performed for 10% of a total 312 rat plasma samples. By using the formula in the method validation section, all results of ISR analysis were calculated to have a RE of less than 20% (Fig. 3, Table 4).

*Pharmacokinetic study and incurred sample reanalysis assessment*

The developed UHPLC-MS/MS method was successfully applied to the quantification of CP, DECP, and KTZ in plasma samples collected according to the sample pretreatment section, and all the data were analyzed us-

Table 3. Matrix effect and extraction recovery of DECP, CP, and KTZ (n=3)

Analyte	Spiked concentration (ng/ml)	Matrix effect	Extraction recovery
DECP	20	$100.10 \pm 0.02\%$	$100.74 \pm 0.87\%$
	80	$106.67 \pm 2.55\%$	$100.04 \pm 1.04\%$
	500	$104.19 \pm 1.42\%$	$100.83 \pm 0.49\%$
CP	20	$96.39 \pm 0.25\%$	$101.82 \pm 3.52\%$
	80	$103.68 \pm 2.70\%$	$99.41 \pm 0.36\%$
	500	$102.79 \pm 1.30\%$	$100.33 \pm 0.88\%$
KTZ	10	$107.57 \pm 1.50\%$	$94.35 \pm 2.31\%$
	40	$105.37 \pm 1.94\%$	$96.40 \pm 0.23\%$
	250	$102.62 \pm 1.64\%$	$97.73 \pm 0.44\%$

Table 4. Stability assessments of DECP, CP, and KTZ under various storage conditions (means $\pm$ SD, n=3)

Analyte	Nominal concentration (ng/ml)	Short term (25ºC for 3 h)			Long term (−80ºC for 3 months)			Three freeze−thaw cycles		
		Measured (ng/ml)	RE (%)	CV (%)	Measured (ng/ml)	RE (%)	CV (%)	Measured (ng/ml)	RE (%)	CV (%)
DECP	20	20.77 ± 0.40	3.85	1.94	22.27 ± 0.84	11.35	3.79	22.49 ± 0.16	12.45	0.70
	80	85.69 ± 1.28	7.11	1.50	91.20 ± 3.46	14.00	3.80	91.19 ± 2.37	13.99	2.60
	500	567.68 ± 80.42	13.54	14.12	563.81 ± 65.07	12.76	11.54	547.55 ± 85.32	9.51	15.58
CP	20	20.57 ± 0.81	2.85	3.92	18.79 ± 0.42	−6.05	2.24	18.68 ± 0.20	−6.60	10.54
	80	84.49 ± 2.05	5.61	2.43	81.16 ± 2.40	1.45	2.96	78.39 ± 1.43	−2.01	18.18
	500	525.40 ± 73.09	5.08	13.91	509.89 ± 68.17	1.98	13.37	490.26 ± 78.18	−1.95	15.95
TKZ	10	9.97 ± 0.23	−0.30	2.28	9.55 ± 0.07	−4.50	0.76	9.57 ± 0.23	−4.30	2.43
	40	42.23 ± 0.76	−0.58	1.80	40.04 ± 0.57	0.10	1.43	39.46 ± 0.44	−1.35	1.11
	250	264.51 ± 38.66	5.80	14.62	259.01 ± 37.39	3.64	14.44	254.65 ± 38.96	1.86	15.30
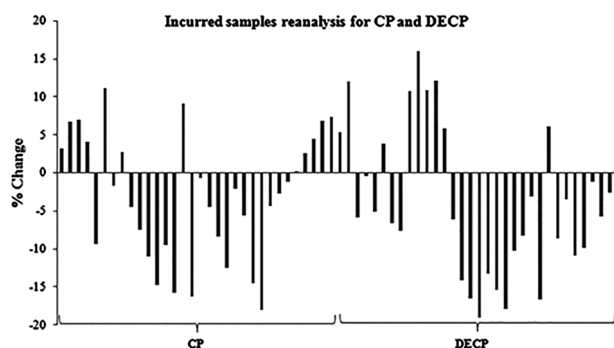
Fig. 3. Graphical representation of the percent change (RE) in CP and DECP concentrations by reanalysis of 32 incurred samples.

ing Drug and Statistics 2.0 (Mathematical Pharmacology Professional Committee of China, Shanghai) for the pharmacokinetic study. Pharmacokinetic parameters, including the area under the plasma-concentration time curve ($AUC_{0-\infty}$), the maximum plasma concentration (C_{max}), and time to achieve the maximum plasma concentration (T_{max}), were obtained directly from the individual plasma concentration-time curves.

The mean plasma concentration-time profile of KTZ in group 0 is shown in Supplementary Fig. 5, and the typical pharmacokinetic parameters of KTZ were as follows: $T_{max}=0.514 \pm 0.399$ h, $C_{max}=2,048.218 \pm 310.733$ ng/ml, $MRT_{0-t}=1.857 \pm 0.193$ h, and $AUC_{0-t}=4,727.037 \pm 1,348.042$ ng*h/ml. Therefore, the CYP3A4 inhibitor KTZ was orally administered to rats 50 min before CP was given on the basis of the pharmacokinetic data and a previous report [17].

The mean plasma concentration-time profiles of CP and DECP for four different groups are depicted in Fig. 4. The corresponding pharmacokinetic parameters of DECP and CP with and without (control) coadministration of KTZ in rats are summarized in Table 5. There was a significant difference in most parameters, including C_{max}, AUC, and MRT, between each KTZ group and control group for DECP ($P<0.05$). It could be concluded that these parameters of DECP all largely decreased after coadministration of KTZ and that they decreased in a dose-dependent manner. Although there was a nonsignificant difference in C_{max} for CP between each KTZ group and control group, AUC increased in a dose-dependent manner when CP was administered in combination with KTZ.
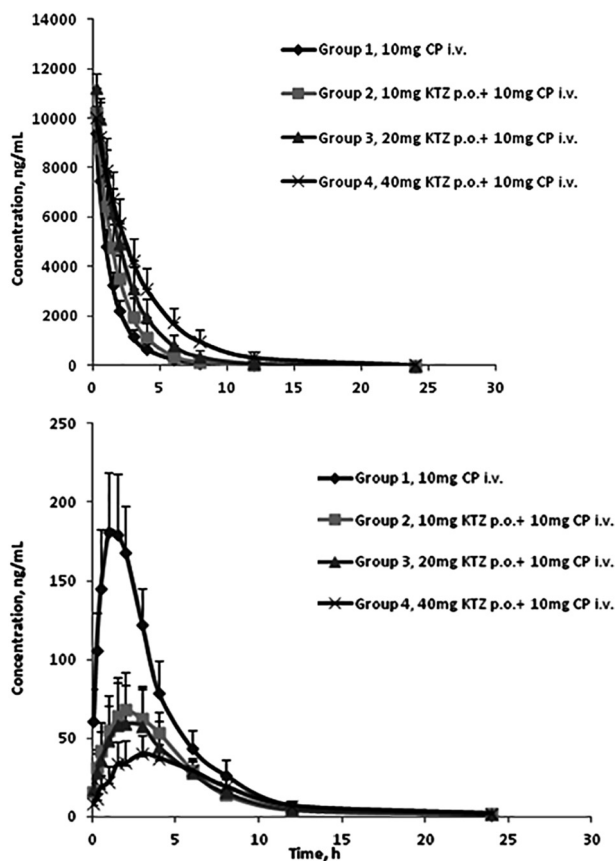
Fig. 4. Concentration-time profiles of CP (A) and DECP (B) in rats with and without (control) coadministration of KTZ (n=6). Group 1 rats were pretreated with 5% CMC-Na and then administered with CP 50 min later (10 mg/kg, i.v.). Group 2 rats were administered CP (10 mg/kg, i.v.) 50 min following an oral dosage of 10 mg/kg KTZ. Group 3 rats were administered CP (10 mg/kg, i.v.) 50 min following an oral dosage of 20 mg/kg KTZ. Group 4 rats were administered CP (10 mg/kg, i.v.) 50 min following an oral dosage of 40 mg/kg KTZ.

Discussion

As one of the dominant enzymes in the liver, characterization the CYP3A4 isoform responsible for drug metabolism is important for potential DDI in humans [31], especially when CYP3A4 significantly contributes to the production of effective and/or toxic drug metabolites. To investigate the effect of concomitant multiple dosing of KTZ on the pharmacokinetics of CP, HLM were selected as the *in vitro* model to calculate the KTZ dosing level for the subsequent rat model study. In our experiment, it was found that administration of KTZ resulted in a dose-dependent decrease in DECP amount and that the IC_{50} value for KTZ concentration was 0.618

μM in HLM. The later Ki values and the Lineweaver-Burk plots analysis revealed that KTZ could be classified as potent noncompetitive inhibitor when its concentration is lower than 3 times the IC_{50} (Fig. 2). Based on these observations, the *in vitro* inhibition model of CYP3A4 activity inhibition by KTZ in HLM led to significant DDI, although CYP3A4 contributed to only about 10% of the metabolism of CP.

For MS condition optimization for analyte detection, the experiment was performed in positive mode due to the higher response than in the negative mode. To develop a rapid and reproducible method, it was of importance to optimize the chromatographic conditions. Organic phases like methanol and acetonitrile were tested, and the acetonitrile-water system showed more powerful separation ability, less interference, and more elution power for the analytes in MS. Moreover, addition of 0.1% formic acid to the mobile phase facilitated achievement of a better symmetric peak shape for MS detection and MS responses. Further improvement for the MS responses and reduced analysis time was achieved through the use of a Waters T3 C18 column (2.1 × 100 mm, 1.7 μm). Finally, satisfactory separation was achieved with a total run time of 4.0 min, and the retention times for DECP, IS, CP, and KTZ were 1.64 min, 2.14 min, 2.67 min, and 2.71 min, respectively.

As the most common preparation techniques used in plasma samples analysis, protein precipitation (PPT), which was applied in our previous experiment [43], was evaluated as the preparation method in this study. It was found that the same one-step 3-fold acetonitrile (containing 0.1% formic acid) precipitation strategy produced satisfactory results for recovery and matrix effect for all analytes when compared with other different precipitants, such as methanol or acetonitrile without addition of formic acid.

This study provides a preliminary view of the pharmacokinetic (PK) DDI between 10 mg/kg of CP and KTZ. The dose of 10 mg/kg for mice was set based on its clinical applications and pre-experimental data. Setting the dose at 10 mg/kg was more accurate, as this dose is used in the treatment of certain diseases. The clinical applications of CP, according to dose, can be summarized as follows: low-dose oral treatments such as 20–50 mg/day for multiple myeloma (MM) and non-Hodgkin's lymphoma [8, 25] and 100–150 mg/day for cryptogenic fibrosing alveolitis and metastatic hormone refractory prostate cancer [24, 29], low-dose intravenous treatments

Table 5. Pharmacokinetic parameters of DECP and CP with and without (control) coadministration of KTZ in rats (means ± SD, n=6)

Parameters	Group 1 (0 mg/kg KTZ)	Group 2 (10 mg/kg KTZ)	Group 3 (20 mg/kg KTZ)	Group 4 (40 mg/kg KTZ)
DECP				
C_{max} (ng/ml)	183.647 ± 36.202	69.347 ± 22.194*	61.432 ± 25.635*	41.138 ± 11.317*
T_{max} (h)	1.25 ± 0.418	2.167 ± 0.931	2.25 ± 0.880	3.667 ± 1.211*
$AUC_{0\to t\,(ng*h/ml)}$	1,129.923 ± 150.102	566.162 ± 157.786*	517.742 ± 167.33*	416.305 ± 88.879*
$AUC_{0\to\infty\,(ng*h/ml)}$	1,171.276 ± 144.209	593.488 ± 159.609*	558.404 ± 162.85*	494.058 ± 96.29*
$MRT_{0-t\,(\mu g/l*h)}$	3.903 ± 0.223	4.899 ± 0.498*	5.315 ± 0.702*	6.542 ± 0.61*
$MRT_{0-\infty\,(\mu g/l*h)}$	4.135 ± 0.253	4.921 ± 0.513*	5.883 ± 1.391*	7.698 ± 0.921*
CP				
C_{max} (ng/ml)	9,420.738 ± 559.763	10,424.558 ± 673.938	11,357.515 ± 544.977	9,599.66 ± 1,763.755
T_{max} (h)	0.194 ± 0.086	0.194 ± 0.086	0.139 ± 0.086	0.347 ± 0.327
$AUC_{0\to t\,(ng*h/ml)}$	1,4844.352 ± 2,082.912	21,096.274 ± 4,654.279	28,704.034 ± 6,136.07*	38,238.601 ± 7,784.632*
$AUC_{0\to\infty\,(ng*h/ml)}$	15,528.318 ± 2,012.778	21,948.945 ± 4,679.703	29,645.827 ± 6,171.944*	39,010.498 ± 7,768.45*
$MRT_{0-t\,(\mu g/l*h)}$	1.699 ± 0.167	1.718 ± 0.357	2.04 ± 0.293	2.649 ± 0.482*
$MRT_{0-\infty\,(\mu g/l*h)}$	1.9 ± 0.345	1.864 ± 0.6	2.116 ± 0.361	2.669 ± 0.505*

C_{max}; maximum plasma concentration, T_{max}; time to C_{max}, AUC; area under the plasma concentration-time curve. *$P<0.05$ means comparison of parameters was significant between the KTZ group and control group.

such as 25 mg/m^2/day (about 40 mg/day) for 28 days for pediatric sarcomas [10] and 2–4 g/m^2 for mobilizing progenitor cells for myeloma [23], and high-dose intravenous treatments such as 120 mg/kg for autologous stem-cell transplantation in MM [14] and 200 mg/kg in aplastic anaemia [37]. The dose of 10 mg/kg was calculated from the 1.67 mg/kg/dose (about 100 mg) for humans, which has been used in single low-dose CP intravenous treatments for many diseases. Furthermore, it was found that determinations for CP and its metabolite DECP were feasible by our established UHPLC-MS/MS method after intravenous treatment with 10 mg/kg of CP. Despite this, the dose of CP for rats will need to be set strictly according to the sorts of treatments applied in the clinic, such as treatments for MM, in future studies.

According to a previous report, several CYP isoforms haven been shown to catalyze C-4 oxidation of CP, CYP2B6 being the main contributor responsible for approximately 45% of the total CP bioactivation, followed by CYP3A4 (25%) and CYP2C9 (12%), while some other P450s, including CYPs 1A1, 2A6, and 2C8, exhibited low CP 4-hydroxylase activity [40]. As a typical 3A4 inhibitor, KTZ was hypothesized to inhibit the dechloroethylation of CP, which was only mediated by CYP3A4. As expected, the plasma concentration of DECP was much lower in the KTZ groups (groups 2–4) after a single dosing than that in the control group, which was thought not to be negligible, while the plasma concentration of CP was slightly higher than that in the control group, without significant differences in the plasma concentration of CP among these groups. In de-

tail, DECP levels (calculated as the mean $AUC_{0-\infty}$ value) in plasma decreased with increasing dose of the CYP3A4 inhibitor KTZ, showing more than a 50% decrease in $AUC_{0-\infty}$ (dosage of CP, 10 mg/kg, i.v.) when coadministration was performed with 40 mg/kg KTZ. Meanwhile, the MRT_{0-t} and $AUC_{0-\infty}$ for CP increased with increasing dose of KTZ, which could be recognized as a compensation change for CP as a consequence of CYP3A4 metabolism insufficiency.

In this study, the production of CAA was reflected by the blood concentration of the accompanying equimolar-yielded metabolite DECP. Actually, it was not possible to determine an accurate concentration of CAA because of its very short half-life and its quick reactive attribute, which enables it to form covalent adducts with nucleophilic thiols or direct Schiff base adducts with nucleophilic nitrogens *in vivo* [6]. In addition, CAA is dangerous when exposed at 45 ppm, which may cause suffering and junctival irritation of the operator [12]. Therefore, CAA assay was abandoned due to its potential toxicity risk. The decrease in DECP plasma concentration disappeared around 10 h after CP administration, which might be attributed to the KTZ concentration decline at this time point (Fig. 4) and/or reversible inhibition on CYP3A4 enzymes by KTZ [18, 41]. This phenomenon was quite consistent with the previous research [38].

It could be concluded that the decrease in CAA in the KTZ groups was caused by an impaired metabolism of CP to DECP through CYP3A4 inhibition, while the CP plasma concentration was insignificantly affected by KTZ. The increase in the MRT_{0-t} (h) of CP in the KTZ

groups reflected the delayed CP metabolism.

Although China's National Center for Adverse Drug Reaction (ADR) showed that oral administration of KTZ had a serious problem with respect to hepatotoxicity at doses in the range of 200–400 mg/day, which accounted for a large proportion among severe cases, the United Kingdom and France have taken more strict measures for its risk management [42]. However, in many studies, multiple KTZ doses were given during the PK sampling, and the doses were set in the range of 200–400 mg/day, in both healthy volunteers and patients [2, 11, 35]. For example, it was reported that coadministration of vene-toclax with KTZ (400 mg once daily for days 5–11) was well tolerated in this a phase 1 study in 12 non-Hodgkin lymphoma patients, with no other serious (grades 3–5) adverse events attributed to study drugs, which could indicate the relative tolerability of KTZ. It was also stated that liver toxicity and injury induced by KTZ were associated with the KTZ dose [15]. KTZ was given to rats in a single dose, not multiple doses, in our study, and no obvious toxicity (indicated by some physiological aspects, data not shown) was observed in the rats, suggesting well toleration of KTZ application within a certain dose range. From another point of view, if there was other CYP3A inhibitors that were not toxic to the important organs such as liver, finding CYP3A inhibitors with relatively fewer side effects should be considered and in investigated in similar DDI experiments. It is also possible that data may become available in the near future from patients treated with CP-based chemotherapy with coadministration of another CYP3A4 inhibitor, as evaluation of outcomes of CP treatment would be of clinical importance even if estimated differences do not attain statistical significance.

There were three limitations for this study. Firstly, no differences were recorded between the groups with or without KTZ. As the animal experiment lasted for only 24 h, little attention was paid to the behaviors of the treated rats, and no undesirable signs of toxicity were observed in any rats in any of the groups. Secondly, we did not perform any *in vitro* and *in vivo* CYP3A4 induction experiments because CYP3A4 inhibition, which could be applied to detoxify CAA-induced side effects, was the most predominant subject in this study. Lastly, the metabolites from the main pathway should have been assayed to further study the other toxicities induced by CP, such as hemorrhagic cystitis and myocardial disorders.

Conclusion

Our *in vitro* HLM modeling approach suggested that a CYP3A4 inhibitor decreased systematic exposure of DECP. Accordingly, an *in vivo* rat modeling approach was applied to comprehensively determine effects of multiple doses of KTZ on both CP and DECP pharmacokinetics in order to elucidate DDI between CP and KTZ. Our results proved a previous hypothesis, i.e., that KTZ can reduce the dechloroethylation of CP both *in vitro* and *in vivo*, indicating that combination usage of a CYP3A4 inhibitor could potentially decrease toxic CAA exposure while not significantly affecting the CP plasma concentration.

Conflict of Interest

None of the authors has any potential conflicts interest related to this manuscript.

Acknowledments

References

1. Abbas, R., Leister, C., El Gaaloul, M., Chalon, S., and Sonnichsen, D. 2012. Ascending single-dose study of the safety profile, tolerability, and pharmacokinetics of bosutinib coadministered with ketoconazole to healthy adult subjects. *Clin. Ther.* 34: 2011–9.e1. [Medline] [CrossRef]
2. Agarwal, S.K., Salem, A.H., Danilov, A.V., Hu, B., Puvvada,

S., Gutierrez, M., Chien, D., Lewis, L.D., and Wong, S.L. 2017. Effect of ketoconazole, a strong CYP3A inhibitor, on the pharmacokinetics of venetoclax, a BCL-2 inhibitor, in patients with non-Hodgkin lymphoma. *Br. J. Clin. Pharmacol.* 83: 846–854. [Medline] [CrossRef]

3. Balap, A., Atre, B., Lohidasan, S., Sinnathambi, A., and Mahadik, K. 2016. Pharmacokinetic and pharmacodynamic herb-drug interaction of Andrographis paniculata (Nees) extract and andrographolide with etoricoxib after oral administration in rats. *J. Ethnopharmacol.* 183: 9–17. [Medline] [CrossRef]

4. Baumann, F., Lorenz, C., Jaehde, U., and Preiss, R. 1999. Determination of cyclophosphamide and its metabolites in human plasma by high-performance liquid chromatography-mass spectrometry. *J. Chromatogr. B Biomed. Sci. Appl.* 729: 297–305. [Medline] [CrossRef]

5. Bohnenstengel, F., Johnson, S., Hofmann, U., Eichelbaum, M., and Kroemer, H.K. 1995. Direct gas chromatographic determination of dechloroethylcyclophosphamide following microsomal incubation of cyclophosphamide. *J. Chromatogr. B Biomed. Appl.* 672: 271–276. [Medline] [CrossRef]

6. Börner, K., Kisro, J., Brüggemann, S.K., Hagenah, W., Peters, S.O., and Wagner, T. 2000. Metabolism of ifosfamide to chloroacetaldehyde contributes to antitumor activity in vivo. *Drug Metab. Dispos.* 28: 573–576. [Medline]

7. Bradford, M.M. 1976. A rapid and sensitive method for the quantitation of microgram quantities of protein utilizing the principle of protein-dye binding. *Anal. Biochem.* 72: 248–254. [Medline] [CrossRef]

8. Buckstein, R., Kerbel, R.S., Shaked, Y., Nayar, R., Foden, C., Turner, R., Lee, C.R., Taylor, D., Zhang, L., Man, S., Baruchel, S., Stempak, D., Bertolini, F., and Crump, M. 2006. High-Dose celecoxib and metronomic "low-dose" cyclophosphamide is an effective and safe therapy in patients with relapsed and refractory aggressive histology non-Hodgkin's lymphoma. *Clin. Cancer Res.* 12: 5190–5198. [Medline] [CrossRef]

9. Cai, F. 2011. Studies on Pharmacokinetics and Compatibility Mechanism of Zishen Pill, Doctor's dissertation (in Chinese), Second Military Medical University.

10. Casanova, M., Ferrari, A., Bisogno, G., Merks, J.H., De Salvo, G.L., Meazza, C., Tettoni, K., Provenzi, M., Mazzarino, I., and Carli, M. 2004. Vinorelbine and low-dose cyclophosphamide in the treatment of pediatric sarcomas: pilot study for the upcoming European Rhabdomyosarcoma Protocol. *Cancer* 101: 1664–1671. [Medline] [CrossRef]

11. Dingemanse, J., Cruz, H.G., Gehin, M., and Hoever, P. 2014. Pharmacokinetic interactions between the orexin receptor antagonist almorexant and the CYP3A4 inhibitors ketoconazole and diltiazem. *J. Pharm. Sci.* 103: 1548–1556. [Medline] [CrossRef]

12. Dow 1962. Personal communication to a ACGIH TLV Committee member from the Dow Chemical Company, Biochemical Research Department.

13. Ekhart, C., Gebretensae, A., Rosing, H., Rodenhuis, S., Beijnen, J.H., and Huitema, A.D. 2007. Simultaneous quantification of cyclophosphamide and its active metabolite 4-hydroxycyclophosphamide in human plasma by high-performance liquid chromatography coupled with electrospray ionization tandem mass spectrometry (LC-MS/MS). *J. Chromatogr. B Analyt. Technol. Biomed. Life Sci.* 854: 345–349. [Medline] [CrossRef]

14. Fenk, R., Schneider, P., Kropff, M., Huenerlituerkoglu, A.N., Steidl, U., Aul, C., Hildebrandt, B., Haas, R., Heyll, A., Kobbe, G., West German Myeloma Study Group 2005. High-dose idarubicin, cyclophosphamide and melphalan as conditioning for autologous stem cell transplantation increases treatment-related mortality in patients with multiple myeloma: results of a randomised study. *Br. J. Haematol.* 130: 588–594. [Medline] [CrossRef]

15. Greenblatt, H.K. and Greenblatt, D.J. 2014. Liver injury associated with ketoconazole: review of the published evidence. *J. Clin. Pharmacol.* 54: 1321–1329. [Medline] [CrossRef]

16. Gupta, A., Singhal, P., Shrivastav, P.S., and Sanyal, M. 2011. Application of a validated ultra performance liquid chromatography-tandem mass spectrometry method for the quantification of darunavir in human plasma for a bioequivalence study in Indian subjects. *J. Chromatogr. B Analyt. Technol. Biomed. Life Sci.* 879: 2443–2453. [Medline] [CrossRef]

17. Hamdy, D.A. and Brocks, D.R. 2010. High performance liquid chromatographic assay for the simultaneous determination of midazolam and ketoconazole in plasma. *J. Pharm. Biomed. Anal.* 53: 617–622. [Medline] [CrossRef]

18. Hamdy, D.A. and Brocks, D.R. 2009. Nonlinear stereoselective pharmacokinetics of ketoconazole in rat after administration of racemate. *Chirality* 21: 704–712. [Medline] [CrossRef]

19. Han, Y.L., Li, D., Ren, B., Jing, G.P., Meng, X.L., Zhou, Z.Y., Yu, Q., Li, Y., Wan, L.L., and Guo, C. 2012. Evaluation of impact of Herba Erigerontis injection, a Chinese herbal prescription, on rat hepatic cytochrome P450 enzymes by cocktail probe drugs. *J. Ethnopharmacol.* 139: 104–109. [Medline] [CrossRef]

20. Huang, Z., Roy, P., and Waxman, D.J. 2000. Role of human liver microsomal CYP3A4 and CYP2B6 in catalyzing N-dechloroethylation of cyclophosphamide and ifosfamide. *Biochem. Pharmacol.* 59: 961–972. [Medline] [CrossRef]

21. Huitema, A.D., Tibben, M.M., Kerbusch, T., Zwikker, J.W., Rodenhuis, S., and Beijnen, J.H. 1998. Simultaneous determination of N,N′,N"-triethylenethiophosphoramide, cyclophosphamide and some of their metabolites in plasma using capillary gas chromatography. *J. Chromatogr. B Biomed. Sci. Appl.* 716: 177–186. [Medline] [CrossRef]

22. Huitema, A.D., Tibben, M.M., Kerbusch, T., Kettenes-van den Bosch, J.J., Rodenhuis, S., and Beijnen, J.H. 2000. Simple and selective determination of the cyclophosphamide metabolite phosphoramide mustard in human plasma using high-performance liquid chromatography. *J. Chromatogr. B Biomed. Sci. Appl.* 745: 345–355. [Medline] [CrossRef]

23. Jantunen, E., Putkonen, M., Nousiainen, T., Pelliniemi, T.T., Mahlamäki, E., and Remes, K. 2003. Low-dose or intermediate-dose cyclophosphamide plus granulocyte colony-stimulating factor for progenitor cell mobilisation in patients with multiple myeloma. *Bone Marrow Transplant.* 31: 347–

351. [Medline] [CrossRef]

24. Johnson, M.A., Kwan, S., Snell, N.J., Nunn, A.J., Dar-byshire, J.H., and Turner-Warwick, M. 1989. Randomised controlled trial comparing prednisolone alone with cyclo-phosphamide and low dose prednisolone in combination in cryptogenic fibrosing alveolitis. *Thorax* 44: 280–288. [Medline] [CrossRef]

25. Kumar, S.K., Vij, R., Noga, S.J., Berg, D., Brent, L., Dollar, L., and Chari, A. 2017. Treating multiple myeloma patients with oral therapies. *Clin. Lymphoma Myeloma Leuk.* 17: 243–251. [Medline] [CrossRef]

26. Liu, M., Su, X., Li, G., Zhao, G., and Zhao, L. 2015. Validated UPLC-MS/MS method for simultaneous determination of simvastatin, simvastatin hydroxy acid and berberine in rat plasma: Application to the drug-drug pharmacokinetic inter-action study of simvastatin combined with berberine after oral administration in rats. *J. Chromatogr. B Analyt. Technol. Biomed. Life Sci.* 1006: 8–15. [Medline] [CrossRef]

27. MacAllister, S.L., Martin-Brisac, N., Lau, V., Yang, K., and O'Brien, P.J. 2013. Acrolein and chloroacetaldehyde: an examination of the cell and cell-free biomarkers of toxicity. *Chem. Biol. Interact.* 202: 259–266. [Medline] [CrossRef]

28. Matsunaga, N., Suzuki, K., Nakanishi, T., Ogawa, M., Im-awaka, H., and Tamai, I. 2015. Modeling approach for mul-tiple transporters-mediated drug-drug interactions in sand-wich-cultured human hepatocytes: effect of cyclosporin A on hepatic disposition of mycophenolic acid phenyl-glucuro-nide. *Drug Metab. Pharmacokinet.* 30: 142–148. [Medline] [CrossRef]

29. Nicolini, A., Mancini, P., Ferrari, P., Anselmi, L., Tartarel-li, G., Bonazzi, V., Carpi, A., and Giardino, R. 2004. Oral low-dose cyclophosphamide in metastatic hormone refrac-tory prostate cancer (MHRPC). *Biomed. Pharmacother.* 58: 447–450. [Medline] [CrossRef]

30. Noh, Y.H., Lim, H.S., Jin, S.J., Kim, M.J., Kim, Y.H., Sung, H.R., Choi, H.Y., and Bae, K.S. 2012. Effects of ketocon-azole and rifampicin on the pharmacokinetics of gemigliptin, a dipeptidyl peptidase-IV inhibitor: a crossover drug-drug interaction study in healthy male Korean volunteers. *Clin. Ther.* 34: 1182–1194. [Medline] [CrossRef]

31. Or, P.M., Lam, F.F., Kwan, Y.W., Cho, C.H., Lau, C.P., Yu, H., Lin, G., Lau, C.B., Fung, K.P., Leung, P.C., and Yeung, J.H. 2012. Effects of Radix Astragali and Radix Rehmanniae, the components of an anti-diabetic foot ulcer herbal formula, on metabolism of model CYP1A2, CYP2C9, CYP2D6, CY-P2E1 and CYP3A4 probe substrates in pooled human liver microsomes and specific CYP isoforms. *Phytomedicine* 19: 535–544. [Medline] [CrossRef]

32. Periasamy, S., Liu, C.T., Chien, S.P., Chen, Y.C., and Liu, M.Y. 2016. Daily sesame oil supplementation mitigates ketoconazole-induced oxidative stress-mediated apoptosis and hepatic injury. *J. Nutr. Biochem.* 37: 67–75. [Medline] [CrossRef]

33. Pont, A., Graybill, J.R., Craven, P.C., Galgiani, J.N., Dis-mukes, W.E., Reitz, R.E., and Stevens, D.A. 1984. High-dose ketoconazole therapy and adrenal and testicular function in humans. *Arch. Intern. Med.* 144: 2150–2153. [Medline]

[CrossRef]

34. Shin, K.H., Kim, B.H., Kim, T.E., Kim, J.W., Yi, S., Yoon, S.H., Cho, J.Y., Shin, S.G., Jang, I.J., and Yu, K.S. 2009. The effects of ketoconazole and rifampicin on the pharma-cokinetics of mirodenafil in healthy Korean male volunteers: an open-label, one-sequence, three-period, three-treatment crossover study. *Clin. Ther.* 31: 3009–3020. [Medline] [CrossRef]

35. Sil Oh, E., Ok Kim, C., Kim, K.H., Kim, Y.N., Kim, C., Lee, J.I., and Park, M.S. 2014. Effect of ketoconazole on lobeg-litazone pharmacokinetics in Korean volunteers. *Clin. Ther.* 36: 1064–1071. [Medline] [CrossRef]

36. Sugar, A.M., Alsip, S.G., Galgiani, J.N., Graybill, J.R., Dis-mukes, W.E., Cloud, G.A., Craven, P.C., and Stevens, D.A. 1987. Pharmacology and toxicity of high-dose ketoconazole. *Antimicrob. Agents Chemother.* 31: 1874–1878. [Medline] [CrossRef]

37. Tisdale, J.F., Dunn, D.E., Geller, N., Plante, M., Nunez, O., Dunbar, C.E., Barrett, A.J., Walsh, T.J., Rosenfeld, S.J., and Young, N.S. 2000. High-dose cyclophosphamide in severe aplastic anaemia: a randomised trial. *Lancet* 356: 1554–1559. [Medline] [CrossRef]

38. Tochitani, T., Yamashita, A., Kouchi, M., Fujii, Y., Matsu-moto, I., Miyawaki, I., Yamada, T., and Funabashi, H. 2016. Changes in plasma concentrations of corticosterone and its precursors after ketoconazole administration in rats: An ap-plication of simultaneous measurement of multiple steroids using LC-MS/MS. *Exp. Toxicol. Pathol.* 68: 125–131. [Medline] [CrossRef]

39. Venkatakrishnan, K., Rader, M., Ramanathan, R.K., Rama-lingam, S., Chen, E., Riordan, W., Trepicchio, W., Cooper, M., Karol, M., von Moltke, L., Neuwirth, R., Egorin, M., and Chatta, G. 2009. Effect of the CYP3A inhibitor ketoconazole on the pharmacokinetics and pharmacodynamics of bortezo-mib in patients with advanced solid tumors: a prospective, multicenter, open-label, randomized, two-way crossover drug-drug interaction study. *Clin. Ther.* 31: 2444–2458. [Medline] [CrossRef]

40. Vredenburg, G., den Braver-Sewradj, S., van Vugt-Lussen-burg, B.M., Vermeulen, N.P., Commandeur, J.N., and Vos, J.C. 2015. Activation of the anticancer drugs cyclophospha-mide and ifosfamide by cytochrome P450 BM3 mutants. *Toxicol. Lett.* 232: 182–192. [Medline] [CrossRef]

41. Yan, Z., Rafferty, B., Caldwell, G.W., and Masucci, J.A. 2002. Rapidly distinguishing reversible and irreversible CYP450 inhibitors by using fluorometric kinetic analyses. *Eur. J. Drug Metab. Pharmacokinet.* 27: 281–287. [Medline] [CrossRef]

42. Yan, J.Y., Nie, X.L., Tao, Q.M., Zhan, S.Y., and Zhang, Y.D. 2013. Ketoconazole associated hepatotoxicity: a systematic review and meta- analysis. *Biomed. Environ. Sci.* 26: 605–610. [Medline]

43. Yang, L., Feng, J., Zhang, F., Jiang, B., Gao, S., and Chen, W. 2014. Fast quantification of cyclophosfamide and its N-dechloroethylated metabolite 2-dechloroethylcyclophospha-mide in human plasma by UHPLC-MS/MS. *Biomed. Chro-matogr.* 28: 1303–1305. [Medline] [CrossRef]